Proceedings of the 9th International Conference on Fluid Flow, Heat and Mass Transfer (FFHMT'22)
Niagara Falls, Canada – June 08-10, 2022
Paper No. 134
DOI: 10.11159/ffhmt22.134

Regeneration of an Aqueous Potassium Lysinate to Capture CO_2 in A Membrane Unit

Nayef Ghasem[1]
[1]Department of Chemical and Petroleum Engineering,
UAE University, Al-Ain city, UAE
nayef@uaeu.ac.ae

Abstract **-** The capture of CO_2 from flue gas and natural gas is essential for the sake of humanity. Aqueous potassium lysinate (LysK) is a suitable solvent utilized in the CO_2 capturing process. Regeneration of the rich Lysk solution is crucial for process continuation and cost-effectiveness. In the present work, a two-dimensional mathematical model that considers both axial and radial diffusion are established to describe the CO_2 elimination from rich potassium lysinate solution. The model describes the LysK regeneration process in a hollow fiber membrane contactor module. The modeling results showed that the carbon dioxide removal ratio is directly proportional to the amount of carbon dioxide present in the solution and the temperature of the solution. The increase in stripping temperature increases the percent CO_2 released from rich solvent.

Keywords**:** Membrane; solvent regeneration; potassium lysinate; CFD; CO_2 capture

1. Introduction

Global warming worries many researchers and countries. Carbon dioxide (CO_2) is the topmost donor to universal heating up. Capture of CO_2 is the primary answer to escape this alarm. Nowadays, the conventional equipment is the absorption of CO_2 in alkanolamine aqueous in a packed bed absorber [1–3]. A substitute solution for the removal of CO_2 from acid gas or natural gas is the amino acid salts such as potassium lysinate which has high reactivity toward CO_2, and they have a comparable functional group as alkanolamine. This solution solves the problems of the alkanolamine solutions. The low volatility, reasonably high surface tension, confrontation to degradation are the key features of those amino salts [4]. Various studied provides the kinetics of these salts [5–11]. Potassium-based absorbents showed a higher reactivity to carbon dioxide than sodium-based solvents [12]. kinetic data for carbon dioxide uptake in several amino salts are studied [6]. Packed and alkanolamine solvents are currently used on the industrial scale [13–15]. Despite the great achievement the packed beds with alkanol amine solvent from being corroded, flooding, regeneration cost [16]. Polymeric hollow fiber liquid-gas membrane contactor (MC) overcomes the packed column drawbacks [2,16,17]. MC is recommended by several researchers for the CO_2 absorption and solvent regeneration (removal of absorbed gas from liquid solution). Membrane material is fabricated from a hydrophobic polymeric material such as polyvinyl fluoride (PVDF) [18]. AAS such as potassium lysinate have the high surface tension [19–23]. Membrane fabricated from hydrophobic material are highly recommended [24–27]. Most of the previous studies focused their attention on modeling and simulating the absorption of CO_2 in MC using the family amine solvents (MEA, DEA). Little care has been given to separating $_{CO2}$ from rich amino acid solvents [15,28–31]. Therefore, in the present work, the stripping of CO_2 from rich LysK solution was mathematically modeled and simulated with Comsol software version 5.6. The model was utilized to investigate the influence of stripping temperatures, CO_2 loading, solvent feed rate in membrane contactor on the stripping efficiency.

2. Model development

The regeneration process of rich aqueous LysK took place in a gas-liquid hollow fiber membrane contactor. Table 1 shows the dimensions of the hollow fiber membrane.

Table 1: Structure of the membrane contactor [1]

Property	value
fiber inside diameter (mm)	0.42
fiber outside diameter (mm)	1.10
Number of fibers	15
Inner surface area (m^2)	5.15×10^{-3}
Diameter of module (mm)	16
Length (mm)	260

Consider isothermal, ideal gas behavior, incompressible fluid, and aqueous potassium lysinate (LysK) is transported in the tube side. The following mass transport equations describe the regeneration process of the chemical of rich LysK. The developed mass transport equations are as follow:

2.1 Tube side

Equation (1) describes the mass balance equations for rich LysK flowing in the tube side:

$$D_{CO_2,t}\frac{1}{r}\left(\frac{\partial}{\partial r}r\left(\frac{\partial C_{CO_2,t}}{\partial r}\right)\right)+D_{CO_2,t}\ \frac{\partial^2 C_{CO_2,t}}{\partial z^2}+R_{CO_2,t}=v_{z,t}\left(\frac{\partial C_{CO_2,t}}{\partial z}\right) \quad (1)$$

$v_{z,t}$ is described by the equation:

$$v_{z,t}=\frac{2Q_t}{n\pi r_1^2}\left(1-\left(\frac{r}{r_1}\right)^2\right) \quad (2)$$

Where Q_t is the liquid volumetric flow rate in the tube side, n is the number of hollow fibers.

Boundary conditions:

at $z = 0$, $C_{CO_2,t}=0$ (initial concentration of CO_2)

at $z = H$, $\frac{\partial^2 C_{CO_2,t}}{\partial z^2}=0$

at $r = 0$, $\frac{\partial C_{CO_2,t}}{\partial r}=0$

at $r = r_1$, $C_{CO_2,t}=m\,C_{CO_2,m}$

The elementary reversible reaction rate is first order concerning rich LysK.

$$r_{CO_2}=k_{-1}C_{LysK} \quad (3)$$

$$k_{LysK}=84822\left(\frac{m^3}{kmol.K}\right)exp\left(-\frac{51kJ/mol}{RT}\right) \quad (4)$$

$$\frac{k_{LysK}}{k_{-1}}=8.2X10^{-18}\,exp\left(\frac{11718}{T}\right) \quad (5)$$

2.2 Membrane side

In this section the transport mechanism in the membrane phase is by diffusion, no convection [32]:

$$D_{CO_2,m}\frac{1}{r}\left(\frac{\partial}{\partial r}r\left(\frac{\partial C_{CO_2,m}}{\partial r}\right)\right)+D_{CO_2},m\frac{\partial^2 C_{CO_2,m}}{\partial z^2}=0 \quad (6)$$

Nitrogen gas component balance of:

$$D_{N_2,m}\frac{1}{r}\left(\frac{\partial}{\partial r}r\left(\frac{\partial C_{N_2,m}}{\partial r}\right)\right)+D_{N_2,m}\frac{\partial^2 C_{N_2,m}}{\partial z^2}=0 \quad (7)$$

Eqns. 9 to 12 designates the suitable boundary conditions of the membrane side ($i: CO_2, N_2$)

at $z = 0,\ \frac{\partial C_{i,m}}{\partial z}=0$

at $z = H,\ \frac{\partial C_{i,m}}{\partial z}=0$

at $r = r_1,\ D_{i,m}\frac{\partial C_{i,m}}{\partial r}=D_{i,t}\frac{\partial C_{i,t}}{\partial r}$

at $r = r_2,\ C_{i,m} = C_{i,s}$

2.2 Shell side

The shell side component mole balance

$$D_{CO_2,s}\frac{1}{r}\left(\frac{\partial}{\partial r}r\left(\frac{\partial C_{CO_2,s}}{\partial r}\right)\right)+D_{CO_2,s}\frac{\partial^2 C_{CO_2,s}}{\partial z}=v_{z,s}\left(\frac{\partial C_{CO_2,s}}{\partial z}\right) \quad (8)$$

$$D_{N_2,s}\frac{1}{r}\left(\frac{\partial}{\partial r}r\left(\frac{\partial C_{N_2,s}}{\partial r}\right)\right)+D_{N_2,s}\frac{\partial^2 C_{N_2,s}}{\partial z}=v_{z,s}\left(\frac{\partial C_{N_2,s}}{\partial z}\right) \quad (9)$$

The shell side's velocity profile [33]

$$v_{z,s}=v_{z,max}\left\{1-\left(\frac{r_2}{r_3}\right)^2\right\}\left\{\frac{\left(\frac{r}{r_3}\right)^2-\left(\frac{r_2}{r_3}\right)^2-2ln\left(\frac{r}{r_2}\right)}{3+\left(\frac{r_2}{r_3}\right)^4-4\left(\frac{r_2}{r_3}\right)^2+4\,ln\left(\frac{r_2}{r_3}\right)}\right\} \quad (10)$$

The applicable boundary conditions are as follows:

at $z = H,\ C_{i,s}=C_{i,0}$ (inlet of sweep gas)

at $z = 0,\ \frac{\partial^2 C_{i,s}}{\partial z^2}=0$

at $r=r_2,\ D_{i,s}\ \frac{\partial C_{i,s}}{\partial r}=D_{i,m}\ \frac{\partial C_{i,m}}{\partial r}$

at $r = r_3,\ \frac{\partial C_{i,s}}{\partial r}=0$

where

$$r_3=r_2\left(\frac{1}{1-\varphi}\right)^{0.5} \quad (11)$$

Eqn. 12 states the void fraction of membrane module (φ):

$$\varphi=\frac{\boldsymbol{R^2-n\,r_2^2}}{\boldsymbol{R^2}} \quad (12)$$

Where the inner radius of module is R, the number fibers is n, and outer radius is r_2. The governing equations were solved simultaneously using the finite element method embedded with the software Comsol 5.6.

3. Results and Discussion

Figure 1 shows the schematic diagram of the CO_2 stripping process using a hollow fiber membrane contactor from hot rich aqueous LysK fed to the membrane module's lumen side, where gaseous nitrogen swept the stripped CO_2 in the module shell side. Figure 2 depicts the 2D mathematical model simulated results.

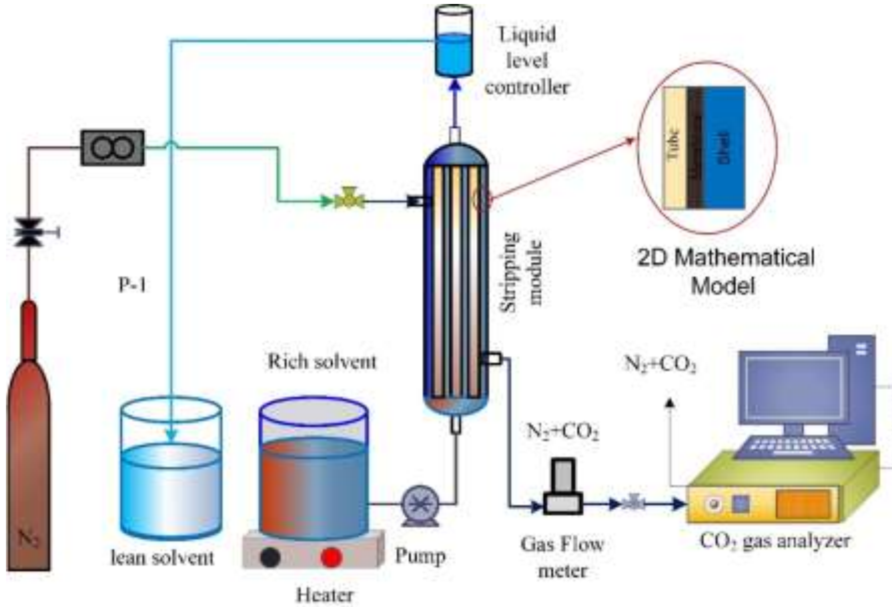

Fig 1: Schematic of the membrane contactor stripping process of CO_2 from aqueous Lysk.

The aqueous amino acid enters the lumen side showing zero CO_2 gaseous concentration; the concentration increased along with the membrane module. Part of the CO_2 diffuses to through the membrane to the shell side, where it has swept out with nitrogen gas. Figure 2 presents the CO_2 surface concentration profile and the direction of the total flux through the membrane unit. The aqueous LysK enters the lumen side of the membrane contactor module with dissolved CO_2 in the solvent during the CO_2 absorption process. The gaseous CO_2 concentration in the rich solvent is negligible. The CO_2 loading presents the dissolved CO_2 concentration in the aqueous LysK. As the hot solvent enters the lumen side, the CO_2 is released from the membrane lumen side and diffuses to the shell side due to the CO_2 concentration gradient. Figure 3 depicts the effect of CO2 loading on the stripping process.

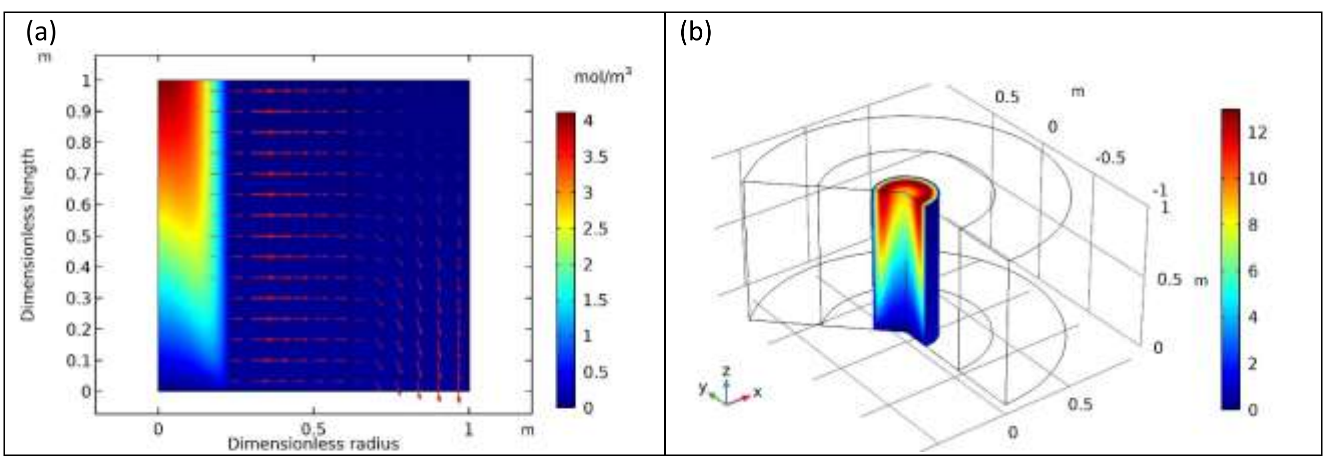

Fig 2: (a) surface concentration the gaseous CO_2 regenerated from LysK across the membrane contactor module, (b) 3D concentration profile of CO_2 in the membrane lumen.

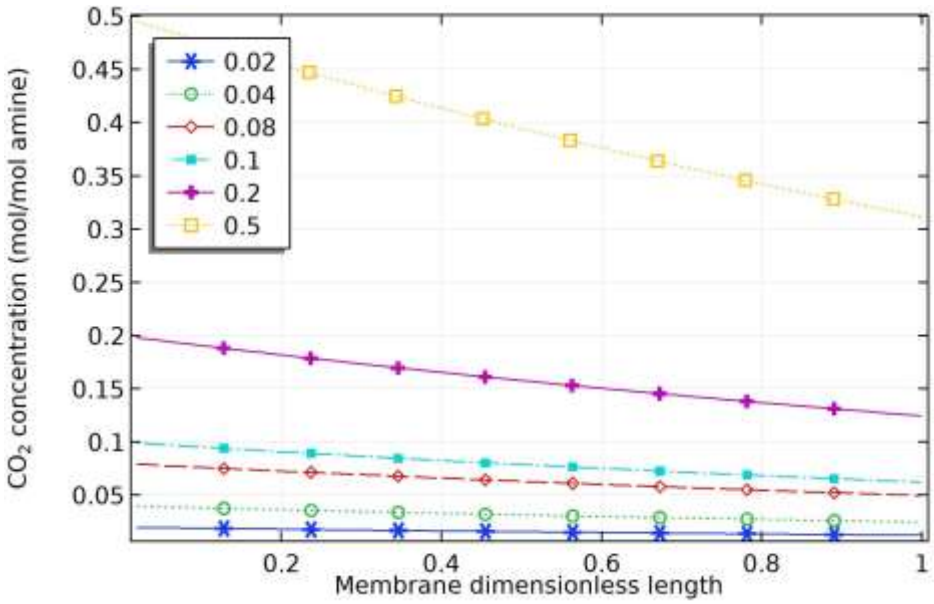

Fig 3: Effect of CO_2 loading in the aqueous LysK on CO_2 concentration profile along the membrane lumen side.

The stripping temperature has a substantial impact on the percent removal of CO2 from the aqueous LysK. As the temperature increased, the percent removal increased, attributed to the increase in the reverse reaction rate constant with increased temperature.

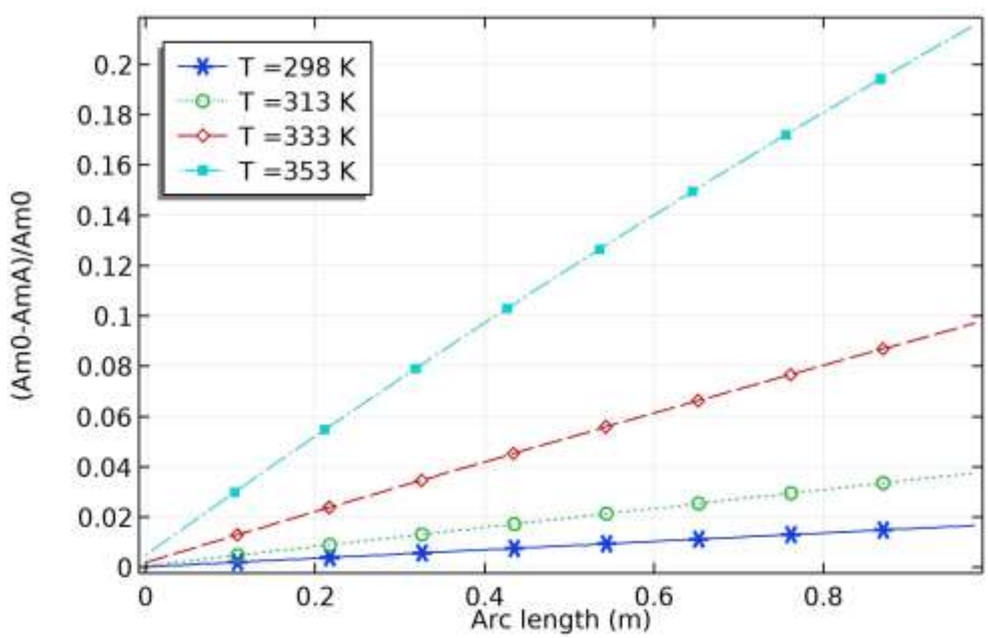

Fig 4: Effect of stripping temperature on the present removal of CO_2 from the aqueous LysK.

Figure 5 shows the CO_2 stripping efficiency at a variable solvent flow rate and a fixed stripping gas rate along the membrane dimensionless length. The stripping efficiency decreased with a high LysK volumetric rate in the lumen membrane. It is attributed to the decrease in solvent residence time and hence the decrease in mass transfer.

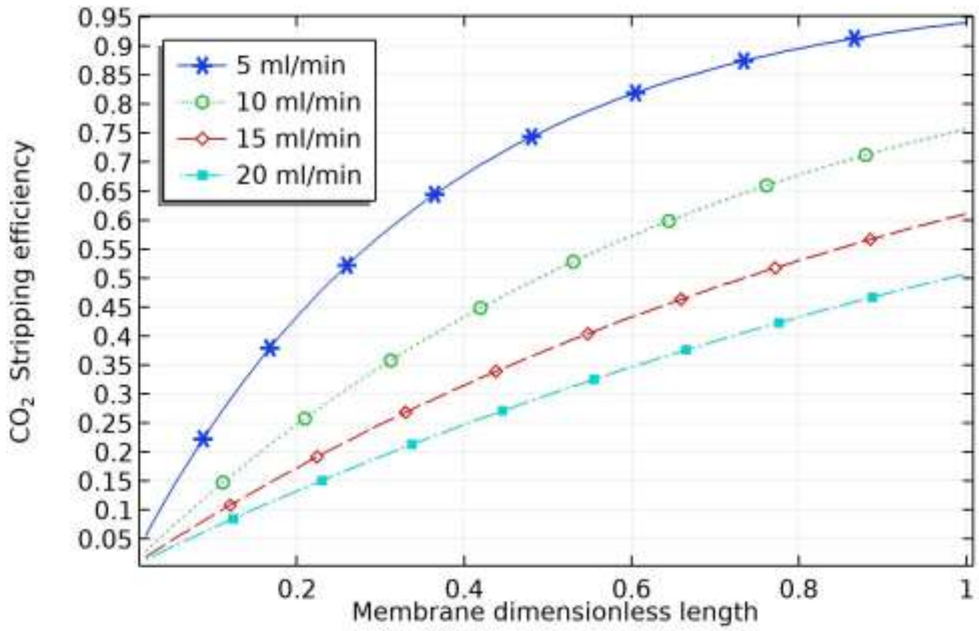

Fig 5: Effect of liquid solvent flow rate at a fixed gas stripped rate on the CO_2 stripping efficiency along the length of the membrane module.

4. Conclusions

The carbon dioxide stripping from the aqueous potassium lysinate solution in a gas-liquid hollow fiber membrane contactor was modeled in a 2D mathematical model and simulated using Comsol version 5.6 software. The model predictions disclosed that percent striping of CO_2 from rich Lysk solution is improved with temperature and increased CO_2 loading. The CO_2 stripping efficiency increased with decreased solvent flow rate.

References

[1] N.A. Rahim, N. Ghasem, M. Al-Marzouqi, Stripping of CO2 from different aqueous solvents using PVDF hollow fiber membrane contacting process, J. Nat. Gas Sci. Eng. 21 (2014) 886–893.

[2] J.L. Li, B.H. Chen, Review of CO2 absorption using chemical solvents in hollow fiber membrane contactors, Sep. Purif. Technol. 41 (2005) 109–122. https://www.sciencedirect.com/science/article/pii/S1383586604002655 (accessed May 6, 2019).

[3] N.A. Rahim, N. Ghasem, M. Al-Marzouqi, Absorption of CO2 from natural gas using different amino acid salt solutions and regeneration using hollow fiber membrane contactors, J. Nat. Gas Sci. Eng. 26 (2015) 108–117.

[4] J. van Holst, G.F. Versteeg, D.W.F. Brilman, J.A. Hogendoorn, Kinetic study of CO2 with various amino acid salts in aqueous solution, Chem. Eng. Sci. 64 (2009) 59–68.

[5] S. Paul, K. Thomsen, Kinetics of absorption of carbon dioxide into aqueous potassium salt of proline, Int. J. Greenh. Gas Control. (2012).

[6] S. Shen, Y.N. Yang, Y. Bian, Y. Zhao, Kinetics of CO2 Absorption into Aqueous Basic Amino Acid Salt: Potassium Salt of Lysine Solution, Environ. Sci. Technol. 50 (2016) 2054–2063.

[7] S. Lee, H.J. Song, S. Maken, J.W. Park, Kinetics of CO2 absorption in aqueous sodium glycinate solutions, Ind. Eng. Chem. Res. 46 (2007) 1578–1583.

[8] A.F. Portugal, J.M. Sousa, F.D. Magalhães, A. Mendes, Solubility of carbon dioxide in aqueous solutions of amino acid salts, Chem. Eng. Sci. 64 (2009) 1993–2002.

[9] A.F. Portugal, F.D. Magalhães, A. Mendes, Carbon dioxide absorption kinetics in potassium threonate, Chem. Eng. Sci. 63 (2008) 3493–3503.

[10] S. Shen, Y. nan Yang, Y. Wang, S. Ren, J. Han, A. Chen, CO 2 absorption into aqueous potassium salts of lysine and proline: Density, viscosity and solubility of CO 2, Fluid Phase Equilib. 399 (2015) 40–49.

[11] S. Mosadegh-Sedghi, S. Félix, A. Mendes, Determination of CO2 Absorption Kinetics in Amino Acid Salts Solutions

Using Membrane Contactors, Int. J. Membr. Sci. Technol. 4 (2017) 8–18.
[12] K. Simons, W. Brilman, H. Mengers, K. Nijmeijer, M. Wessling, Kinetics of CO2 absorption in aqueous sarcosine salt solutions: Influence of concentration, temperature, and CO2 loading, Ind. Eng. Chem. Res. 49 (2010) 9693–9702.
[13] S.A. Hashemifard, H. Ahmadi, A.F. Ismail, A. Moarefian, M.S. Abdullah, The effect of heat treatment on hollow fiber membrane contactor for CO2 stripping, Sep. Purif. Technol. 223 (2019) 186–195.
[14] K.E. Zanganeh, A. Shafeen, C. Salvador, CO2 Capture and Development of an Advanced Pilot-Scale Cryogenic Separation and Compression Unit, Energy Procedia. 1 (2009) 247–252.
[15] A.T. Nakhjiri, A. Heydarinasab, O. Bakhtiari, T. Mohammadi, Modeling and simulation of CO2 separation from CO2/CH4 gaseous mixture using potassium glycinate, potassium argininate and sodium hydroxide liquid absorbents in the hollow fiber membrane contactor, J. Environ. Chem. Eng. 6 (2018) 1500–1511.
[16] D. Demontigny, P. Tontiwachwuthikul, A. Chakma, Comparing the absorption performance of packed columns and membrane contactors, Ind. Eng. Chem. Res. 44 (2005) 5726–5732.
[17] S. Karoor, K.K. Sirkar, Gas Absorption Studies in Microporous Hollow Fiber Membrane Modules, Ind. Eng. Chem. Res. 32 (1993) 674–684.
[18] S.A. Hashemifard, H. Ahmadi, A.F. Ismail, A. Moarefian, M.S. Abdullah, The effect of heat treatment on hollow fiber membrane contactor for CO2 stripping, Sep. Purif. Technol. 223 (2019) 186–195.
[19] S. Masoumi, M.R. Rahimpour, M. Mehdipour, Removal of carbon dioxide by aqueous amino acid salts using hollow fiber membrane contactors, J. CO2 Util. (2016).
[20] S. Shen, Y. Zhao, Y. Bian, Y. Wang, H. Guo, H. Li, CO2 absorption using aqueous potassium lysinate solutions: Vapor – liquid equilibrium data and modelling, J. Chem. Thermodyn. 115 (2017) 209–220.
[21] K.M.S. Salvinder, H. Zabiri, S.A. Taqvi, M. Ramasamy, F. Isa, N.E.M. Rozali, H. Suleman, A. Maulud, A.M. Shariff, An overview on control strategies for CO2 capture using absorption/stripping system, Chem. Eng. Res. Des. 147 (2019) 319–337.
[22] S. Yan, Q. Cui, L. Xu, T. Tu, Q. He, Reducing CO 2 regeneration heat requirement through waste heat recovery from hot stripping gas using nanoporous ceramic membrane, Int. J. Greenh. Gas Control. (2019).
[23] F. Seibert, I. Wilson, C. Lewis, G. Rochelle, Effective Gas/Liquid Contact Area of Packing for CO2 absoprtion/stripping, in: Greenh. Gas Control Technol., 2005: pp. 1925–1928.
[24] R. Naim, A.F. Ismail, Effect of polymer concentration on the structure and performance of PEI hollow fiber membrane contactor for CO2 stripping, J. Hazard. Mater. 250–251 (2013) 354–361.
[25] M. Rahbari-Sisakht, D. Rana, T. Matsuura, D. Emadzadeh, M. Padaki, A.F. Ismail, Study on CO2 stripping from water through novel surface modified PVDF hollow fiber membrane contactor, Chem. Eng. J. 246 (2014) 306–310.
[26] R. Naim, K.C.C. Khulbe, A.F.F. Ismail, T. Matsuura, Characterization of PVDF hollow fiber membrane for CO2 stripping by atomic force microscopy analysis, Sep. Purif. Technol. 109 (2013) 98–106.
[27] G. Bakeri, A.F. Ismail, M. Shariaty-Niassar, T. Matsuura, Effect of polymer concentration on the structure and performance of polyetherimide hollow fiber membranes, J. Memb. Sci. 363 (2010) 103–111.
[28] X. Yang, R.J. Rees, W. Conway, G. Puxty, Q. Yang, D.A. Winkler, Computational Modeling and Simulation of CO 2 Capture by Aqueous Amines, Chem. Rev. 117 (2017) 9524–9593.
[29] M.R. Sohrabi, A. Marjani, S. Moradi, M. Davallo, S. Shirazian, Mathematical modeling and numerical simulation of CO2 transport through hollow-fiber membranes, Appl. Math. Model. 35 (2011) 174–188.
[30] F.J. Valdés, M.R. Hernández, L. Catalá, A. Marcilla, Estimation of CO 2 stripping/CO 2 microalgae consumption ratios in a bubble column photobioreactor using the analysis of the pH profiles. Application to Nannochloropsis oculata microalgae culture, Bioresour. Technol. 119 (2012) 1–6.
[31] S. Eslami, S.M. Mousavi, S. Danesh, H. Banazadeh, Modeling and simulation of CO2 removal from power plant flue gas by PG solution in a hollow fiber membrane contactor, Adv. Eng. Softw. 42 (2011) 612–620.
[32] N. Hajilary, M. Rezakazemi, CFD modeling of CO2 capture by water-based nanofluids using hollow fiber membrane contactor, Int. J. Greenh. Gas Control. 77 (2018) 88–95.
[33] J. Happel, Viscous flow relative to arrays of cylinders, AIChE J. 5 (1959) 174–177.